

governing complexes, whereas the VB approach does contain within it additional features which allow deviations from a smooth relationship.

What comments may we make on the question of transition-state structure on the basis of our results and analysis? Arguing by analogy with our results for reaction complexes, it would appear that the Hammond postulate, which strictly speaking only refers to transition-state structure in highly exothermic or endothermic reactions, is substantiated. On the other hand, the differential extension of the Hammond postulate, sometimes termed the Leffler-Hammond postulate^{25c} (but often erroneously also termed the Hammond postulate), may not be universally valid. Stabilization of reactants in a given reaction may not necessarily mean that the transition state will be more product-like.

Conclusions

The results presented in this paper provide further support for a structural postulate for complexes¹⁴ analogous to the Hammond postulate⁵ for transition states, namely, when two sets of reactants [(AB + C) or (A + BC)] interact to form a common stable complex (A-B-C), the complex will generally resemble the set of reactants of lower energy. The differential analogue of this postulate is not invariably true, i.e., stabilization of one set of reactants does not necessarily result in increasing resemblance of the complex structure to these reactants. Both of these results are readily rationalized in terms of a configuration valence bond model.

Acknowledgment. We thank Dr. S. Shaik for helpful comments.

Why UO₂²⁺ Is Linear and Isoelectronic ThO₂ Is Bent

Willard R. Wadt

Contribution from the Theoretical Division, Los Alamos National Laboratory, Los Alamos, New Mexico 87545. Received February 9, 1981

Abstract: The isoelectronic species UO₂²⁺ and ThO₂ possess very different geometries, namely, UO₂²⁺ is linear while ThO₂ is strongly bent ($\theta_{\text{expt}} = 122 \pm 2^\circ$). Relativistic effective core potential (RECP) calculations using Hartree-Fock wave functions and double-zeta-plus-polarization quality basis sets were performed to determine the origin of this difference. The RECP calculations correctly predict the linear and bent geometries of UO₂²⁺ and ThO₂ ($\theta_{\text{calcd}} = 118^\circ$). The Th-O bond length, which is not known experimentally, is calculated to be 1.91 Å. Analysis of the results shows that the difference in geometries for UO₂²⁺ and ThO₂ has its origin in the relative ordering of the 5f and 6d levels. For uranium the 5f levels are lower and dominate the back-bonding from the oxygen in UO₂²⁺, while for thorium the 6d levels are lower and dominate the back-bonding in ThO₂. Finally, the 5f levels prefer linear geometries, while the 6d prefer bent geometries, hence, the difference between UO₂²⁺ and ThO₂. The relative ordering of the 5f and 6d levels has a profound effect.

The uranyl cation (UO₂²⁺) is very familiar and well-studied moiety in actinide chemistry. It always appears in a trans, i.e., linear, configuration in uranyl complexes. Given the linearity of UO₂²⁺ it is surprising that matrix isolation studies¹ indicate that the isoelectronic species ThO₂ possesses a bent geometry ($\theta = 122 \pm 2^\circ$). It is natural to ask whether the significant difference in geometry indicates a significant difference in the bonding of UO₂²⁺ and ThO₂. To shed light on this question we have performed calculations on UO₂²⁺ and ThO₂ using ab initio Hartree-Fock wave functions based on relativistic effective potentials.² Finally, the results on UO₂²⁺ will be useful for comparison to the extended Hückel calculations of Tatsumi and Hoffmann.³ The latter indicate that the nonvalence 6p orbitals of uranium play a key role in determining the linear geometry of UO₂²⁺.

Computational Details

The relativistic effective core potential (RECP) method has been discussed in detail elsewhere.² Briefly, the core electrons are replaced with a one-electron effective potential based on numerical relativistic Hartree-Fock atomic wave functions,⁴ which include effects arising from the Darwin and mass-velocity terms. For uranium we employed the RECP previously used in calculations on UF₆⁵ and UF₅.⁶ It is based on U³⁺ atomic wave functions and replaces all but the outer 11 electrons, i.e., 6s²6p⁶5f³. For thorium we determined an RECP based on Th⁰ atomic wave functions, which replaced all but the outer 10 electrons, i.e.,

Table I. Representation of the Relativistic Th⁰ Effective Core Potential in Terms of Gaussian Functions of the Form $d_k r^{n_k} e^{-\zeta_k r^2}$ ($N_c = 80$, the Number of Core Electrons)

n_k	ζ_k	d_k	n_k	ζ_k	d_k
$(U_g - N_c/r)r^2$			$(U_s - U_g)g^2$		
0	39.7460	-0.215583	0	102.2215	2.631316
1	120.8967	-24.125688	1	32.1822	36.168565
1	17.1550	-37.429045	1	7.6879	40.379434
2	6.5275	-46.429080	2	2.6445	40.337168
2	2.3245	-14.403078	2	0.4673	11.401892
2	0.7593	-1.156695			
$(U_d - U_g)r^2$			$(U_d - U_g)r^2$		
0	133.8067	4.697283	0	300.1223	2.912226
1	72.6419	69.214991	1	132.6264	73.921541
2	33.2173	401.032676	2	66.9945	464.679400
2	9.2374	158.353053	2	22.0007	264.072748
2	1.2414	93.227065	2	5.9121	84.016104
2	1.0867	-61.096221	2	1.1499	18.143108
$(U_f - U_g)r^2$					
0	92.3245	3.937853			
1	28.3994	62.024430			
2	9.9343	132.317163			
2	2.0660	13.093309			
2	1.6609	-7.882653			

6p⁶6d²7s². The f and g components of the RECP were determined from the 6p⁶5f¹6d¹7s² and 5g¹ configurations, respectively, by using core orbitals frozen from the 6p⁶6d²7s² configuration. The parameters for the Gaussian fit to the RECP are given in Table I. The only deviation from past derivations of RECP's is that the procedure proposed by Christiansen et al.⁷ and modified by Hay⁸

(1) S. D. Gabelnick, G. T. Reedy, and M. G. Chasanov, *J. Chem. Phys.*, **60**, 1167 (1974).

(2) L. R. Kahn, P. J. Hay, and R. D. Cowan, *J. Chem. Phys.*, **68**, 2386 (1978).

(3) K. Tatsumi and R. Hoffmann, *Inorg. Chem.*, **19**, 2656 (1980).

(4) R. D. Cowan and D. C. Griffin, *J. Opt. Soc. Am.*, **66**, 1010 (1976).

(5) P. J. Hay, W. R. Wadt, L. R. Kahn, R. C. Raffanetti, and D. C. Phillips, *J. Chem. Phys.*, **71**, 1767 (1979).

(6) W. R. Wadt and P. J. Hay, *J. Am. Chem. Soc.*, **101**, 5198 (1979).

(7) P. A. Christiansen, Y. S. Lee, and K. S. Pitzer, *J. Chem. Phys.*, **71**, 4445 (1979).

Table II. Atomic Basis Set Used for Thorium

exponent	contraction coefficient	
	s	
0.1628		<u>1.0</u>
0.09045		<u>1.0</u>
0.02721		<u>1.0</u>
	p	
1.163		-0.29324
0.5092		<u>0.86703</u>
0.1870		<u>1.0</u>
0.07		<u>1.0</u>
	d	
0.3244		<u>1.0</u>
0.1185		0.48949
0.04389		0.18699
	f	
3.336		0.22601
1.209		<u>0.47592</u>
0.3969		<u>0.45058</u>
0.1105		0.22520

Table III. Total SCF Energies (in au) for the Ground States of UO_2^{2+} and ThO_2 as a Function of Bond Length, R (in Å),^a and Bond Angle, θ

R	θ , deg					
	180	170	120			
(a) UO_2^{2+} (Energies Relative to -201 au)						
1.85	-0.9364					
1.73	-1.0176	-1.0150	-0.9409			
1.67	-1.1403					
1.64	-1.0449	-1.0420	-0.9571			
1.61	-1.0441					
1.49	-0.9663					
R	θ , deg					
	180	135	124	120	116	105
(b) ThO_2 (Energies Relative to -172 au)						
1.80	-0.4250	-0.4434		-0.4477		-0.4466
1.89				-0.4654		
1.92	-0.4434	-0.4621	-0.4656	-0.4661	-0.4641	-0.4452
1.95				-0.4641		
2.04				-0.4452		-0.4390

^a That is, the two bond lengths are taken to be equal.

was used to determine the pseudoorbitals. Calculations with a uranium potential derived with the modified procedure⁸ led to comparable results for UO_2^{2+} .

A (4s4p3d4f) set of Gaussian primitives contracted to [3s3p2d2f] was used for uranium,⁵ while a (3s4p3d4f)/[3s3p2d2f] set given in Table II was used for thorium. Two contractions were tested for the thorium d and f functions: (1) the standard double-zeta contraction in which the inner two or three primitives are contracted together and the outermost primitive is free and (2) a contraction in which the inner one or two primitives were contracted and the outer two primitives contracted together. Calculations indicated that the second contraction scheme (cf. Table II) lowered the energy by 0.60 eV for ThO_2 ($R_1 = R_2 = 1.80$ Å, $\theta = 120^\circ$). Hence, the second scheme was used. For oxygen a standard (9s5p1d)/[3s2p1d] set⁹ was employed. Finally, spin-orbit effects on the orbital energies were introduced as described elsewhere^{5,10} by using an effective one-electron, one-center spin-orbit operator. The values of the parameters, λ_i , used in evaluating the spin-orbit matrix elements were taken from previous work for uranium⁵ and oxygen,¹⁰ while new values were determined

(8) P. J. Hay, unpublished results.

(9) T. H. Dunning, Jr. and P. J. Hay, in "Modern Theoretical Chemistry", Vol. III, H. F. Schaefer III, Ed., Plenum, New York, 1977.

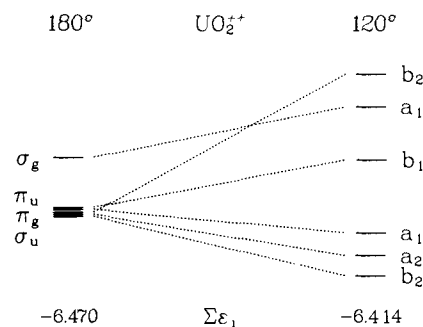
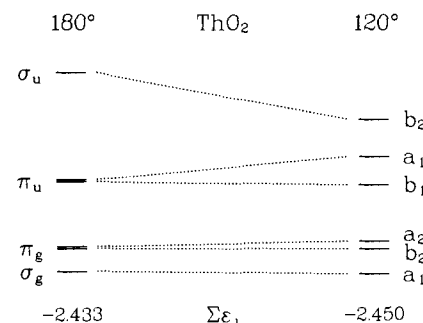
(10) J. S. Cohen, W. R. Wadt, and P. J. Hay, *J. Chem. Phys.*, **71**, 2955 (1979).

Table IV. Optimal Ground-State Geometries for UO_2^{2+} and ThO_2 Obtained with Hartree-Fock Wave Functions. Bond Lengths Were Forced to be Equal

	R , Å	θ , deg
UO_2^{2+}	1.63	180
ThO_2	1.91	118

Table V. Orbital Energies (in au) and Uranium 6d and 5f Mulliken Populations for UO_2^{2+} with $R = 1.64$ Å

orbital	$\theta = 180^\circ$			$\theta = 120^\circ$			
	energy	6d	5f	energy	6d	5f	
σ_g	-1.056	0.13		b_2	-1.015	0.10	0.33
π_u	-1.081		0.28	a_1	-1.031	0.12	0.15
	-1.081		0.28	b_1	-1.057	0.06	0.16
π_g	-1.084	0.21		a_1	-1.093	0.11	0.12
	-1.084	0.21		a_2	-1.104	0.14	0.09
σ_u	-1.084		0.57	b_2	-1.114	0.06	0.21

Figure 1. Walsh diagram for UO_2^{2+} ($R = 1.64$ Å) for six highest occupied orbitals together with the sum of the orbital energies, $\sum \epsilon_i$ in au.Figure 2. Walsh diagram for ThO_2 ($R = 1.92$ Å) for six highest occupied orbitals together with the sum of the orbital energies, $\sum \epsilon_i$ in au.

for thorium, namely, 12562, 858.4, and 48.90 for the 6p, 6d, and 5f orbitals, respectively.

Results

In optimizing the geometry of UO_2^{2+} and ThO_2 , the bond lengths were forced to be equal, i.e., C_{2v} and $D_{\infty h}$ geometries were considered. A list of the SCF total energies is given in Table III, while the results of the optimization are given in Table IV. Since we are considering a bare, gas-phase uranyl cation, there are no experimental data on the geometry. However, UO_2^{2+} always appears in a trans configuration in complexes; so the predicted linear geometry is in agreement with experiment. The U-O bond distance depends strongly on the ligand, ranging from 1.6–2.0 Å,¹¹ so that the theoretical prediction is reasonable. Moreover, one would expect an especially short U-O bond in the absence of other ligands or counterions. For ThO_2 the predicted bond angle is in very good agreement with the spectroscopic value of $122 \pm 2^\circ$.¹ There are no experimental determinations of the Th-O bond length so that the present calculation represents the most reliable value

(11) F. A. Cotton and G. Wilkinson, "Advanced Inorganic Chemistry", 3rd ed., Interscience, New York, 1972, pp 1088–1089.

Table VI. Orbital Energies (in au) and Thorium 6d and 5f Mulliken Populations for ThO_2 with $R = 1.92 \text{ \AA}$

orbital	$\theta = 180^\circ$		$\theta = 120^\circ$				
	energy	6d	5f	orbital energy	6d	5f	
σ_u	-0.324		0.25	b_2	-0.354	0.08	0.10
π_u	-0.393		0.12	a_1	-0.378	0.10	0.05
	-0.393		0.12	b_1	-0.396	0.08	0.07
π_g	-0.436	0.21		a_2	-0.431	0.17	0.04
	-0.436	0.21		b_2	-0.437	0.12	0.05
σ_g	-0.451	0.13		a_1	-0.453	0.14	0.02

Table VII. Total Mulliken Populations for UO_2^{2+} ($R = 1.64 \text{ \AA}$) and ThO_2 ($R = 1.92 \text{ \AA}$) at $\theta = 180$ and 120° ($q =$ atomic charge)

		uranium or thorium					oxygen			
		s^a					p			
		d	f	q	s	p	d	q		
UO_2^{2+}	180°	2.03	5.81	1.20	2.41	2.54	3.90	4.32	0.05	-0.27
	120°	2.07	5.92	1.36	2.25	2.46	3.90	4.29	0.05	-0.23
ThO_2	180°	0.01	6.07	1.19	1.06	1.67	3.88	4.94	0.02	-0.84
	120°	0.00	6.04	1.55	0.73	1.68	3.88	4.95	0.02	-0.84

^a Note that 6s electrons are treated explicitly for uranium and are included in the RECP for thorium.

Table VIII. Vertical Ionization Potentials (in eV) for UO_2^{2+} Obtained from Koopmans' Theorem (KT), Koopmans' Theorem Plus Spin-Orbit (KT + S-O), and Δ SCF Calculations for $R = 1.64 \text{ \AA}$, $\theta = 180^\circ$

	Δ SCF	KT	KT + S-O	
$1^2\Sigma_g^+$	27.27	28.73	28.73	$1(1/2)_g$
$1^2\Sigma_u^+$	27.79	29.51	28.93	$1(1/2)_u$
$1^2\Pi_g$	28.48	29.50	29.47	$1(3/2)_g$
			29.53	$2(1/2)_g$
$1^2\Pi_u$	28.53	29.41	29.16	$1(3/2)_u$
			29.94	$2(1/2)_u$

available for this quantity. Finally, spectroscopic measurements give a bond length of 1.84 \AA for ThO_2 ,¹² which is slightly shorter than the calculated ThO_2 bond length of 1.91 \AA as would be expected for ionic metal-oxygen bonds.

Walsh diagrams¹³ for the six highest occupied orbitals of UO_2^{2+} and ThO_2 are given in Figures 1 and 2. We see that the Walsh diagrams give the correct prediction that UO_2^{2+} is linear and ThO_2 is bent. The orbital energies along with Mulliken populations of the metal 5f and 6d orbitals are listed in Tables V and VI. Total Mulliken populations and atomic charges are given in Table VII. Finally, in Tables VIII and IX the effects of spin-orbit coupling and SCF relaxation on the vertical ionization potentials are considered for UO_2^{2+} and ThO_2 .

Discussion

The RECP calculations correctly predict that UO_2^{2+} is linear while isoelectronic ThO_2 is strongly bent. This is reassuring, but leaves unanswered the more important question, namely, why these two isoelectronic molecules possess such different geometries. Tatsumi and Hoffmann³ proposed that UO_2^{2+} was linear because of the interplay between the uranium 6p and 5f levels and the oxygen 2p levels. Specifically, their extended Hückel calculations indicate a significant interaction between the U 6p and the O 2p orbitals, destabilizing the $2p\sigma_u$ orbital, which is, in turn, stabilized by the U 5f orbitals. However, the same mechanism would predict ThO_2 is linear; so further discussion is required.

The 6p levels in Th^0 and U^0 are comparable in energy. Since the uranium is more highly ionized in UO_2^{2+} than thorium in ThO_2 (cf. Table VII), the 6p levels will be higher in ThO_2 and hence closer in energy to the oxygen 2p levels. Consequently, one would expect a stronger interaction between the $Th(6p)$ and the σ_u combination of the O(2p) for linear ThO_2 . In fact, the 6p

Table IX. Vertical Ionization Potentials (in eV) for ThO_2 Obtained from Koopmans' Theorem (KT), Koopmans' Theorem Plus Spin-Orbit (KT + S-O), and Δ SCF Calculations for $R = 1.92 \text{ \AA}$, $\theta = 120^\circ$

	Δ SCF	KT	KT+S-O	
1^2B_2	8.35	9.65	9.39	1Γ
1^2A_1	8.96	10.30	10.21	2Γ
1^2B_1	9.46	10.76	10.87	3Γ
1^2A_2	10.50	11.75	11.73	4Γ
2^2B_2		11.89	11.90	5Γ
2^2A_1		12.32	12.34	6Γ

Table X. Atomic Orbital Energies (in au) for Uranium and Thorium Based on Relativistic Hartree-Fock Calculations⁴

atom	configuration	$\epsilon(5f)$	$\epsilon(6d)$
U^0	$[Rn]5f^3 6d^1 7s^2$	-0.331	-0.187
U^{2+}	$[Rn]5f^3 6d^1$	-0.801	-0.639
Th^0	$[Rn]6d^2 7s^2$		-0.235
Th^{2+}	$[Rn]5f^1 6d^1$	-0.231	-0.216

character in the highest σ_u is 15% in linear ThO_2 ($R = 1.92 \text{ \AA}$) compared to 9% in linear UO_2^{2+} ($R = 1.64 \text{ \AA}$). The difference would be much more striking if we compared the molecules by using similar bond lengths. For example, the 6p character increases to 23% for ThO_2 ($R = 1.80 \text{ \AA}$) and decreases to 6% for UO_2^{2+} ($R = 1.73 \text{ \AA}$). Therefore, one would expect the σ_u orbital formed from the O(2p) levels to be destabilized more by the interaction with the 6p in ThO_2 than UO_2^{2+} . In turn, the less stable σ_u orbital of ThO_2 should interact strongly and favorably with the empty 5f orbital, leading to a linear geometry for ThO_2 . Since ThO_2 is bent, the effect of the uranium 6p orbitals appears to be less than previously thought.

As a further test we performed calculations on UO_2^{2+} using an earlier RECP for uranium of Kahn et al.² This RECP was based on U^0 atomic wave functions and included the 6s and 6p levels in the core. According to the results of Tatsumi and Hoffmann,³ calculations with this uranium RECP should lead to a nonlinear UO_2^{2+} , since the 6p levels are not explicitly present. However, the calculations actually predict a linear geometry for UO_2^{2+} ; so the 6p levels cannot be playing a key role.

Simple electrostatic arguments cannot explain the difference in geometry between UO_2^{2+} and ThO_2 . From Table VII we see that the oxygens are considerably more ionic in ThO_2 than UO_2^{2+} , so that electrostatic forces, which favor linear geometries, should be more important for ThO_2 . Consequently, we must consider some other interaction.

Examining the tabulated results, a number of significant differences between UO_2^{2+} and ThO_2 are apparent. First the ordering of the highest occupied orbitals are different (cf. Tables V and VI). This is especially evident for the linear geometries. Second, the population of the 5f orbitals is much greater in UO_2^{2+} than ThO_2 . The origin of these differences is readily discerned in terms of a simple picture of the bonding in these compounds.

To start let us assume that the bonding in UO_2^{2+} and ThO_2 is completely ionic, i.e., each oxygen removing two electrons from the metal, leaving just the radon core or $[U^{6+}(O^{2-})_2]^{2+}$ and $[Th^{4+}(O^{2-})_2]$. Examination of the Mulliken atomic charges in Table VII shows that this is an extreme picture. To moderate the ionic picture we must consider back-bonding into the empty low-lying metal orbitals, namely, the 5f and 6d.

Table X shows the relative energies of the 5f and 6d orbitals for various states of uranium and thorium. For uranium the 5f level is significantly lower than the 6d, while for thorium the 6d is slightly lower. This is not surprising since as one moves from left to right across the actinide series the 5f level decreases relative to the 6d as indicated by the series of ground-state valence configurations: $Th(6d^2 7s^2)$, $Pa(5f^3 6d^1 7s^2)$, $U(5f^3 6d^1 7s^2)$, $Pu(5f^5 7s^2)$. Therefore, one expects the 5f orbitals to participate much more than the 6d in back-bonding in UO_2^{2+} and the 6d orbitals to participate a bit more than the 5f in back-bonding in ThO_2 . These expectations are borne out by the results in Table VII (cf. results for 180° , in particular).

(12) K. P. Huber and G. Herzberg, "Constants of Diatomic Molecules," Van Nostrand Reinhold, New York, 1979, pp 640-641.

(13) A. D. Walsh, *J. Chem. Soc.*, 2266 (1953).

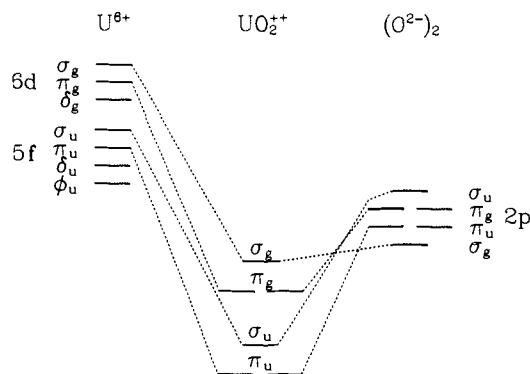


Figure 3. Schematic orbital energy diagram for linear UO_2^{2+} using an ionic model for the bonding.

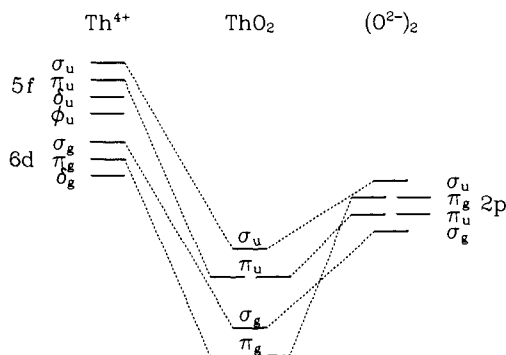


Figure 4. Schematic orbital energy diagram for linear ThO_2 using an ionic model for the bonding.

The relative ordering of the 5f and 6d levels can also be used to explain the differences in the ordering of the molecular levels. In Figure 3, we have indicated in a schematic fashion the ordering of the occupied molecular orbitals arising from the oxygen 2p levels for $(\text{O}^{2-})_2$ as well as the empty 5f and 6d levels on uranium. The ordering within the 5f and 6d levels is determined by simple crystal field effects for a linear geometry. In $D_{\infty h}$ the 5f levels can interact only with the σ_u and π_u orbitals, while the 6d levels can interact only with the σ_g and π_g . Since the 5f levels are lower, one expects the σ_u and π_u to be stabilized relative to the σ_g and π_g by back-bonding. This explains why the σ_u is actually lower than the σ_g (cf. Table V). However, these simple arguments fail to explain the position of the π_u , which one would expect to be lower than the π_g .

Figure 4 illustrates the situation for ThO_2 in which the 6d levels are below the 5f. Comparison of Figure 4 with Table VI or Figure 2 shows that the predicted orbital ordering is correct. In ThO_2 the σ_g and π_g , which can mix with the 6d levels, are stabilized relative to the σ_u and π_u . Consequently, the σ_u is the highest occupied orbital in ThO_2 , while the σ_g is the highest in UO_2^{2+} .

As shown in Figures 1 and 2, the highest occupied orbitals for UO_2^{2+} and ThO_2 behave in opposite fashion upon bending, so that the Walsh diagram leads to the correct prediction of the respective geometries. Bending the molecules enables all of the highest occupied orbitals to mix in 5f and 6d character as indicated in Tables V and VI. However, the total Mulliken populations in Table VII reveal an interesting fact. For both UO_2^{2+} and ThO_2 , bending leads to increased participation of the 6d levels in back-bonding with a concomitant reduction in the use of the 5f levels. This implies that the 5f levels are more effective in back-bonding for linear geometries, while the 6d levels are more effective for bent geometries. This fact combined with the relative ordering of the 5f and 6d levels explains the different geometries preferred by the isoelectronic species UO_2^{2+} and ThO_2 . For uranium the 5f levels are lower than the 6d; they dominate the back-bonding in UO_2^{2+} and lead to a linear geometry. For thorium the 6d levels are lower than the 5f; they dominate the back-bonding in ThO_2 and lead to a bent geometry.

Before considering the effects of spin-orbit coupling and SCF relaxation on the calculated ionization potentials, there is one more difference between the 5f and 6d levels worth noting. For both UO_2^{2+} and ThO_2 in linear configurations, back-bonding into the 5f orbitals is much greater for the σ_u than the π_u , while back-bonding into the 6d orbitals is much greater for the π_g than the σ_g (cf. Tables V and VI). The former is expected since one normally expects the overlap between the $2p_\sigma$ and $5f_\sigma$ orbitals to be greater than $2p_\pi$ and $5f_\pi$. However, the latter result indicates that the $6d_\pi-2p_\pi$ overlap is greater than the $6d_\sigma-2p_\sigma$. This is indeed the case, and the reason is that the 6d orbital is quite large. In fact, the expectation value of r for the atomic 6d orbital i.e., $\langle 6d|r|6d\rangle$, is more than 80% of the bond length in UO_2^{2+} and ThO_2 . Consequently, the $6d_\sigma$ extends beyond the oxygen nucleus and has significant overlap with the negative lobe of the $2p_\sigma$ orbital behind the oxygen. This, of course, reduces the $6d_\sigma-2p_\sigma$ overlap. The 5f orbital, on the other hand, is much smaller with an expectation value of r equal to roughly 50% of the bond length in UO_2^{2+} and ThO_2 . Consequently, the $5f_\sigma$ orbital does not extend significantly beyond the oxygen nucleus, so that the $5f_\sigma-2p_\sigma$ overlap is larger than the $5f_\pi-2p_\pi$. This result points out one of the most interesting aspects of bonding in early actinide compounds, namely, the participation of orbitals with different principal quantum numbers, i.e., 5f and 6d.

Since uranium and thorium are very heavy atoms, spin-orbit effects are significant. The spin-orbit parameters determined by atomic relativistic Hartree-Fock calculations⁴ on uranium and thorium are, respectively, 1879 and 973.8 cm^{-1} for the 5f, 2945 and 1621 cm^{-1} for the 6d, and 48 871 and 41 058 cm^{-1} for the 6p. The effects of spin-orbit coupling on the Koopmans' theorem ionization energies are shown in Tables VIII and IX. Since the highest lying orbitals are predominantly O(2p) in character the changes are generally not large. The largest effects occur for those states arising from ionization out of orbitals that have significant 6p character, i.e., $1^2\Sigma_u^+$ and $1^2\Pi_u$ in UO_2^{2+} and 1^2B_2 in ThO_2 . Similarly, for those states arising from ionization out of orbitals that have no 6p character by symmetry, the effects are small, i.e., $1^2\Sigma_g^+$ and $1^2\Pi_g$ in UO_2^{2+} and 1^2A_2 in ThO_2 . For UO_2^{2+} the spin-orbit effects are sufficiently large to alter the predicted state ordering. In particular, the splitting between the $1^2\Sigma_g^+$ and $1^2\Sigma_u^+$ is greatly reduced. Tables VIII and IX also show the effects of allowing the ionized state to relax by performing an SCF calculation on the UO_2^{3+} or ThO_2^+ state. For ThO_2 the relaxation effects are comparable for the four states considered (~ 1.3 eV). However, for UO_2^{2+} there is considerable variation in the relaxation, from 0.88 eV to 1.72 eV. The origin of the variation may be found in the significant differences in the amount of uranium character in the ionized orbital (cf. Table V). Mulliken population analyses of the states of UO_2^{3+} indicate comparable charge distributions of $\text{U}^{2.92+}(\text{O}^{0.04+})_2$ for all four states which corresponds to removing 0.38 e^- from uranium and 0.31 e^- from each oxygen. To the extent that the Koopmans' theorem ion differs from this charge distribution there will be significant relaxation. For the $1^2\Sigma_u^+$ state the ionized σ_u orbitals has 67% uranium character (5f and 6p) so that there is considerable relaxation with charge transferred from the O(2p) to the U(5f). However, for the $1^2\Sigma_g^+$ state the ionized σ_g orbital has only 14% uranium character (6d and 6s); so again there is considerable relaxation but this time charge is transferred from the U(6d) to the O(2p). The relaxation for the $1^2\Pi_g$ and $1^2\Pi_u$ states is less since the ionized π_g and π_u orbitals possess 21% and 31% uranium character which is closer to the final result that the uranium loses roughly 0.38 e^- .

If one combines the effects of spin-orbit and relaxation, it is apparent that the $1(1/2)_g$ and $1(1/2)_u$ states will be nearly degenerate. Therefore, we cannot confidently predict which is lower. This is an appropriate point to compare with the previous local exchange calculations on UO_2^{2+} . There is considerable disagreement among the Dirac-Slater¹⁴ and two relativistic $X\alpha$ calculations^{15,16} as to the ordering of the highest levels arising

primarily from the O(2p) levels. The present calculations only add to the confusion, since they lead to another different ordering. Nevertheless, the situation is not as bad as it seems, since all of these states cluster in a 1-3-eV band. The experimental XPS spectrum of UO_2CO_3 by Veal et al.¹⁷ shows a strong 2-eV wide band which corresponds to the states arising from the O(2p) levels. Therefore, experiment cannot resolve the discrepancies among the theoretical calculations. On the other hand, there is reasonable agreement among all the calculations and experiment as to the position and nature of the higher states, namely, those arising from the U(6p) and O(2s). All the calculations show a strong mixing between the U(6p) and O(2s) because of their proximity as well as the significant effect of spin-orbit coupling on the U(6p). An extensive discussion of this problem is given by Wood et al.¹⁶

The situation for ThO_2 is very similar, namely, a broad band corresponding to the cluster of states arising from the O(2p), followed by the states arising from the Th(6p) and O(2s), which again are strongly mixed. This prediction is borne out by the XPS spectra of ThO_2 .¹⁸

Conclusions

Relativistic effective core potential (RECP) calculations using double-zeta-plus-polarization quality basis sets correctly predict

(15) C. Y. Yang, K. H. Johnson, and J. A. Horsley, *J. Chem. Phys.*, **68**, 1001 (1978).

(16) J. H. Wood, M. Boring, and S. B. Woodruff, *J. Chem. Phys.*, **75**, 5225 (1981).

(17) B. W. Veal, D. J. Lam, W. T. Carnall, and H. R. Hoekstra, *Phys. Rev. B*, **12**, 5651 (1975).

(18) B. W. Veal and D. J. Lam, *Phys. Rev. B*, **10**, 4902 (1974).

that UO_2^{2+} possesses a linear geometry while isoelectronic ThO_2 is strongly bent with a bond angle of 118° (experiment¹ gives $122 \pm 2^\circ$). The calculated Th-O bond length of 1.91 Å is the most reliable value for this experimentally undetermined quantity. Moreover, the theoretical value differs considerably from recent estimates (1.80 Å)¹⁹ used in calculating thermodynamic data.

Analysis of the results shows that the 6p levels do not play a key role in determining the linear geometry of UO_2^{2+} as proposed by Tatsumi and Hoffmann.³ Instead we find that the difference in geometries for UO_2^{2+} and ThO_2 has its origin in the relative ordering of the 5f and 6d levels. For uranium the 5f levels are lower and dominate the back-bonding from the oxygen in UO_2^{2+} , while for thorium the 6d levels are lower and dominate the back-bonding in ThO_2 . Finally, the 5f levels prefer linear geometries, while the 6d prefer bent geometries; hence, the difference which exists between UO_2^{2+} and ThO_2 . So it is clear that relative ordering of the 5f and 6d levels has a profound effect. This unique feature of two valence levels possessing different principal quantum numbers makes the electronic structure and chemistry of the early actinides a fascinating subject.

Acknowledgment. I enjoyed stimulating discussions with Jeff Hay and Mike Boring. This work was performed under the auspices of the U.S. Department of Energy.

(19) D. W. Green, *J. Nucl. Mater.* **88**, 51 (1980).

Polyacene Dianion Crystal Lattice Energies and Thermodynamic Stabilities: The Quantitative Effect of Aromaticity

Gerald R. Stevenson,* Steven S. Zigler, and Richard C. Reiter

Contribution from the Illinois State University, Department of Chemistry, Normal, Illinois 61761. Received March 30, 1981

Abstract: A calorimeter interfaced with a data acquisition system has been used to measure the heats evolved from the reactions of solid sodium polyacene dianion salts with water. These heats were utilized in a thermochemical cycle to obtain the thermodynamic stabilities (heats of formation) of the salts. For all of the polyacene dianion salts including those from anthracene, tetracene, pentacene, etc., the heats of formation from the polyacene and sodium metal were found to be negative. Electron-electron repulsion energies (E_{rep}) were calculated for each of the dianions. The calculated results could then be used with the experimental heats of formation to obtain the actual crystal lattice energies for the salts. For all of the systems studied the crystal lattice energies were found to be between 400 and 440 kcal/mol. Assuming a similar crystal lattice energy for the sodium benzene dianion ($\text{Na}^+_2\text{Bz}^{2-}$), its heat of formation from benzene and sodium metal was found to be very endothermic (+96 kcal/mol). Much of this endothermicity is due to the antiaromatic nature of the benzene dianion. The enthalpy of transferring two electrons from the benzene dianion to the antiaromatic (planar) cyclooctatetraene neutral molecule to form benzene and the cyclooctatetraene dianion is about -177 kcal/mol.

Chemists have known for some time that it is easier to add extra electrons to 4n π -electron annulenes than to aromatic systems. The dianions of both [8]annulene¹ and [16]annulene² are readily generated via alkali metal reduction of the neutral molecular systems. However, the dianion of benzene (a 4n + 2 π -electron annulene) is still unknown. The dianions of fused polyaromatic systems can be generated but with more difficulty than those for

the 4n π -electron annulenes.³ The reason for the less negative reduction potentials of the 4n π -electron annulenes than of the aromatic system is the fact that the addition of two electrons leads to an aromatic annulene in the 4n π -electron systems and to a divergence from aromatic character in the aromatic systems.

In a previous communication we reported that the solid sodium salts of both [8]annulene and anthracene are stable while main-

(1) Allendoerfer, R. D.; Rieger, P. H. *J. Am. Chem. Soc.* **1965**, *87*, 2336.

(2) Oth, J. F. M.; Baumann, H.; Gilles, J. M.; Schroder, G. *J. Am. Chem. Soc.* **1972**, *94*, 3498.

(3) Sommerdijk, J. L.; De Boer, E. In "Ions and Ion Pairs in Organic Reactions", Szwarc, M., Ed.; Intersciences Publishers: New York, 1972; Vol. 1, pp 363-374.